MedCrave
Step into the World of Research

Physics & Astronomy International Journal

Research Article

Open Access

CrossMark

# Four-dimensional algorithm for studying geological features on mars using high-resolution stereo camera

## Abstract

In this work is developed a new four-dimensional algorithm for studying geological features on Mars using a high-resolution stereo camera. The 4-D B-spline model has been implemented to reconstruct 4-D geological features such as Mars craters. The B-spline solid algorithm is implemented to simultaneously trace tag craters in sequences of high-resolution stereo camera slices by completely identifying B-spline surfaces which ally themselves with attached pixels. The study shows that B-spline can identify flow patterns from larger craters to the small crater. The Marghany 4-D algorithm of great polygon pattern flows is reconstructed using a 4-D B-spline. In conclusion, integration between the Marghany 4-D B-spline algorithm and the high-resolution stereo camera shows excellent promises for implementing Marghany 4-D algorithm in remote sensing applications.

**Keywords:** Four-dimensional algorithm, B-spline model, Mars craters, stereo camera, Marghany algorithm.

Volume 6 Issue 2 - 2022

Maged Marghany
Global Geoinformation Sdn. Bhd, Malaysia

**Correspondence:** Maged Marghany, Global Geoinformation Sdn. Bhd, Kuala Lumpur, Malaysia,
Email magedupm@hotmail.com

**Received:** March 14, 2022 | **Published:** May 03, 2022

## Introduction

In recent times, there is an excessive consideration toward MARS. Man, in actual fact, is considering a wide settlement on the MARS surface as was done on the Earth, previously. This is because in the solar system Earth is the utmost MARS like planet. As stated by Martin et al.,[1] the preliminary geologic investigations of Mars initiated from the ground-based telescopic studies once Mars and the Earth are next to each other in the solar system. Furthermore, the spatial resolution issued to be approximately 100 km owing to the supreme prosaic atmospheric environments. Therefore, these investigations exposed two noteworthy surface mechanisms (i) optimistic and (ii) shady zones, convoyed by inclusive depictions of the polar caps growing and deterioration, in sequences. The optimistic and shady zones are systematized into the sequences of albedo forms, which have been equally endless for no less than hundreds of years, excluding for generally short-span periodic or discrepancies because of dust storms. Assumptions on the configuration of the MARS surface involved on oxidized iron (Fe3+), constructed on the tremendously red colour of the optimistic zones, were created to be analogous to that of countless oxidized land-dwelling soils and desert rocks.[2,3] In the 1960s and 1970s, spectroscopic inspections were instigated to enumerate the colour variances amongst innumerable districts and specified that the shady districts encompass the mineral pyroxene, relating them to a volcanic cause.[4] In the 1980s and 1990s, ground-based and HST telescopic exploration have exposed unfluctuating further indication for mineralogic erraticism among and between optimistic and shady zones on the surface of Mars.

In the mid-1960s, therefore, satellite remote sensing explorations have been instigated that provoked our visualization of the geological structure of the surface of Mars, which demonstrated that Mars was as soon as abundant geologically and climatically shreds of evidence than it is at the present time. Preliminary, telescopic explorations of Mars converged on the sorting of surface albedo forms and inspecting surface and atmospheric changeability. In this respect, the geological evidence was problematic to acquire from diagrams and photos, which had the lowest spatial resolutions of hundreds of kilometers in which any information is impossible to be retrieved.[4]

Rencz,[4] stated that numerous photographic and/or spectroscopic data for the surface of MARS of the south polar cap have been delivered by the spacecraft through the Mariner 4, 6, and 7, respectively. Therefore, spacecraft the Mariner 9 and Viking missions delivered visible, thermal-IR data and spectroscopic analyzed data, which illustrated evidence of volcanic eruptions for hundreds of years on the surface of MARS. These volcanic activities were formed the recent geologically different patterns on MARS. Conceivably most attractive was the finding of the Mars dendritic valley network systems, which are made up of the activity of fluid extreme flows on the Mars surface.[5] Consequently, the trials aboard the dual Viking Lander tasks from 1976 to 1980 were chiefly devised to investigate for confirmation of organic resources, which may perhaps specify the occurrence of recent or historical life on Mars. In 1989, the Phobos-2 spacecraft which is based on spectroscopic data of both near-IR and thermal-IR images, which were delivered information on the Mars surface thermophysical possessions and the Martian surface mineralogy for constrained zones.[4,6]

The progress of infrared sensor arrays is the function of both near-IR and mid-IR wavelengths, which are compiled of indium and antimony (InSb) substrates. Further, infrared sensor arrays have remarkable achievement in completing a high signal-to-noise ratio (SNR), which delivers high-quality images. In addition, the high dynamic range for telescopic and spacecraft imaging can be implemented in different applications. Therefore, the red planet has dominated by an abundant quantity of mineralogy, which is only can be explored by spectroscopic remote sensing. In essence, the spectroscopic is the function of (i) spectra of thermal emission; (ii) spectra of visible reflectance, and (iii) spectra of both gamma-ray and X-ray.

Consistent with Evans et al.[7] and Yin et al.,[8] analytical statistics on the plenty of precise mineralogical in the remotest deposits of a red planet surface can be investigated using both gamma-ray and X-ray. In this understanding, X-ray and charged cosmic rays can penetrate deeply up to numerous centimetres of the surface of the red planet in which X-ray spectrum can react with specific subsurface elements such as Na and Mg. Consequently, secondary radiation based on the

concept of the black body can be distinguished through semiconductor and scintillator devices which are mainly based on the speculations of X-ray spectra intensity is proportional to gamma-ray energies and gas-filled intensities. In this view, both rock-made-up minerals such as Al, Si, P, and S and radioactive elements such as K, Th, U, and hydrogen can be traced by spectroscopic remote sensing techniques.

According to the above perspective, Burns[9] and Gaffey et al.,[10] stated the few microns of crystallinity and mineralogy of red planet surface can be detected by spectroscopy reflectance spectra signature. To this end, the sunlight spectra reflectance is taken into account to measure the amount of mineralogy on the Mars surface. However, spectra reflectance is restricted to a certain wavelength once the Sun radiation energy is great. In other words, the spectra thermal radiation range of 0.3 to 3.5 μm that emitted from the object is smaller than the reflected one. In this regard, the evidence of continental basaltic lava flows on the surface of the red planet is mainly traced by thermal emission, which indicates the abundance of thermal rocks on the Martian surface.[11,12] Numerous studies, therefore, are conducted on the red planet surface topography using the Hubble Space Telescope (HST). However, these investigations are delimited to terrain and landforms features. In this view, HST is a great NASA space observation device in which it involves advanced technology observation levels of the Spitzer Space Telescope; the Chandra X-ray; and the Compton Gamma Ray space sensors.[13] HST, moreover, involves an advanced sensor that functions with a great spectral range of energy range between 20 keV to 30 GeV. The spacecraft shuttles are embedded in a specific range of X-rays and gamma-rays, which are the core electromagnetic spectra exploited for planetary monitoring and surveying, for instance, the MARS. In this regard, both spectra relinquish detailed target measurement and geographical universal locations data in the solar system. Further, the physical object brightness in the nucleus, arms, and halo of a spiral galaxy can be precisely distinguished by both gamma-ray and X-ray from the surrounding galaxy. Nevertheless, in the timescales of a few seconds and minutes, the detected target from the spiral galaxy can be vanished as a tiny point in space.

In the last decade, the MARS express mission is well established by the efforts of the European Space Agency (ESA). Its name was derived because of its quick build compared to any other comparable planetary mission. Mars Express was launched on track for the Red Planet, voyaging at a speed of 10 800 km/hour, relative to the Earth. The mission is expected at perusing the red planet's atmosphere; ionosphere; surface and subsurface. In this regard, the red planet surface is investigated using a High-resolution Stereo Camera (HRSC) while visible and Infrared Mineralogical Mapping Spectrometer (OMEGA) is mainly for mineral rock studies. However, Mars subsurface is mainly observed by Subsurface Sounding Radar Altimeter (MARSIS). Consequently, 3-D geological structural features of the surface, crust, and interior of the red planet can be delivered by HRSC. On the other hand, Ultraviolet and Infrared Atmospheric Spectrometer (SPICAM); Energetic Neutral Atoms Analyzer (ASPERA); and Planetary Fourier Spectrometer (PFS) devices are mainly exploited to investigate the fluctuation of Mars ionosphere and atmosphere; respectively.

Now, the significant question is: in what logic can the similar algebraic formations reveal spaces considering 2-, 3- and 4-D? The novelty of this investigation is to reconstruct Mars geological features such as carter in a 4-D using a high-resolution stereo camera (HRSC) by developing a new algorithm is named by Marghany four-dimensional algorithm (M-4D). The main hypothesis is that 4-D is coded into 3-D of HRSC. To reconstruct 4-D from 3-D data, the 4-D spline is implemented in the stereo-image of HRSC data. Therefore, Marghany's four-dimensional algorithm (M-4D) is aimed to be the specific 4-D algorithm in constructing carters in space-time dimension.

## Data sets

Germany's space agency DLR has contributed to ESA in delivering HRSC sensors as the most significant support to the Mars Express mission. The foremost demonstrable of this mission, which arrive at Mars in late 2003 for searching the water and any vanishing civilization as significant signs of life. The HRSC is fixed on the spacecraft, which was specifically designed to investigate the red planet surface in high resolution. This perhaps aids in precise information regarding geological and mineralogical features besides the structure of the Martian atmosphere and its dealings with the surrounding universal galaxy (DLR, 2015). The HRSC, consequently, is delivered 3-D high tomography resolution of the red planet in the resolution of 10 meters in the perfect full-colour images. In some circumstances, HRSC can deliver the image in 2 m-resolution in specific red planet regions. In addition, HRSC can fuse different resolution images into two sorts of data because of sensor involves an ultra-high-resolution telephoto lens. Therefore, there is a great possibility to imaging any object on Mars within 2 to 3 m-resolution owing to the Super Resolution Channel (SRC) being involved in HRSC (Figure 1).

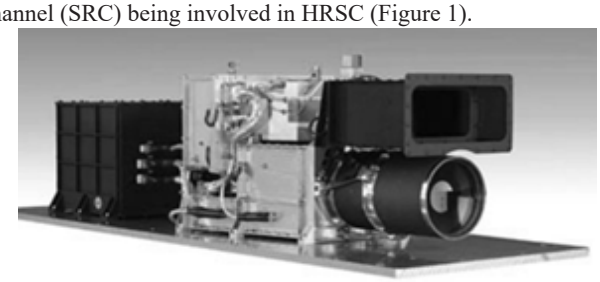

**Figure 1** High-resolution stereo camera (HRSC).

The HRSC camera system has two main cameras: (i) the High-Resolution Stereo head; and (ii) the SRC head. The High-Resolution Stereo head comprises nine CCD line sensors framed analogous behind a lens. On the other hand, the SRC head is constituted of a CCD array sensor and mirror telephoto lens. In this circumstance, an individual sensor accounts for the matching object on the Mars surface at a diverse angle. Three-dimensional images, therefore, are engendered by sequences of five strip images. Consequently, multi-spectral images are created using the residual four of the nine-line sensors are fit out with superior colour filters (Figure 2).

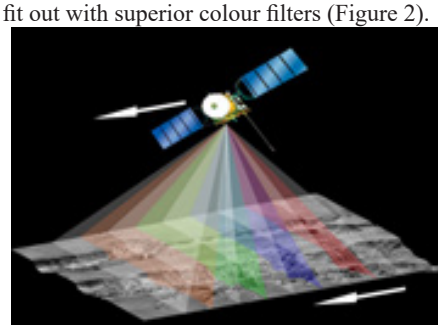

**Figure 2** HRSC camera scanning system.

The advance of this mission is that the spacecraft was located away from Mars by an approximate distance of 270 Km, which helps to deliver 9 image strips for every of the 5184 seven-micron square pixels with 12 m-resolution. In this view, the image has a 52 km swath and the lowest strip dimension of 300 Km, which relies on the spacecraft's data loading and transmission size. The Super Resolution Channel (SRC) is treated as a telephoto glass. At the epicentre, it offers

**Citation:** Marghany M. Four-dimensional algorithm for studying geological features on mars using high-resolution stereo camera. *Phys Astron Int J.* 2022;6(2):38–42. DOI: 10.15406/paij.2022.06.00248

coverage images of 2.3 Km *x* by 2.3 Km wide in the centre of the data strips. On the other hand, the surface information is recorded with a 2.3 m-resolution per pixel, which delivers precisely high-resolution geological features acquired by the stereo head.

## Marghany four-dimensional algorithm

Now, the question is: how to encode 2-D or 3-D sequences HRSC data into 4-D? Along with Marghany,[14] the 4-D reconstructions of remotely sensed data must be considered as periodical fluctuation data. In other words, time series of sequences of remote sensing data over a similar space region must be implemented to reconstruct 4-D frame fluctuations of any object. To this end, encode the 3-D cartesian vector coordinates into interval μ of 0, and one. This mathematically can be expressed as constrained set vectors $|\vec{u}\rangle,|\vec{v}\rangle,|\vec{w}\rangle \in \left[|0\rangle,|1\rangle\right]$. To transfer this 3-D vector set into 4-D surface consider that transitional surface set vector as $|\vec{u}\rangle,|\vec{v}\rangle,|\vec{w}\rangle \in \left[|S\rangle,|t\rangle\right]$ where $S|\vec{u}\rangle,S|\vec{v}\rangle,S|\vec{w}\rangle \in \left[|\vec{x}\rangle,|\vec{y}\rangle,|\vec{z}\rangle,\langle t|\right]$. In this regard, assume that number of solid geometrical transferred frame surfaces of $S_0|\vec{u}\rangle,S_0|\vec{v}\rangle,S_o|\vec{w}\rangle,|t_0\rangle$ to $S_n|\vec{u}\rangle,S_n|\vec{v}\rangle,S_n|\vec{w}\rangle,|t_n\rangle$ are considered and then interpreted mathematically as given by:

$$\vec{V}\left[|S\rangle|t\rangle\right] = S_n|\vec{u}\rangle,S_n|\vec{v}\rangle,S_n|\vec{w}\rangle,|t_n\rangle - S_0|\vec{u}\rangle,S_0|\vec{v}\rangle,S_o|\vec{w}\rangle,|t_0\rangle \quad (1.0)$$

Equation 1.0 demonstrates the fluctuations frames dynamic motions as considering the time is the fourth dimension. In this sense, the periodic frame numbers are about 6 frames, which consumed 588 seconds to be transferred from the original frame to reference periodical frames $|t_n\rangle$. Therefore, the surface of $|S_n\rangle$ turned into reference transferred curve $|C_n,t\rangle$ of the fitted matrix $|\vec{N}_{1\times n}\rangle \cdot |\vec{P}_{n\times 3}\rangle$, which is expressed by:

$$|\vec{C}(t)\rangle = |\vec{N}_{1\times n}\rangle \cdot |\vec{P}_{n\times 3}\rangle = \left(|\vec{N}_{0,p}(t)\rangle \;\; |\vec{N}_{1,p}(t)\rangle \;\; \ldots \;\; |\vec{N}_{n-1,p}(t)\rangle\right) \begin{pmatrix} |\vec{P}_{0,x}\rangle & |\vec{P}_{0,y}\rangle & |\vec{P}_{0,z}\rangle \\ |\vec{P}_{1,x}\rangle & |\vec{P}_{1,y}\rangle & |\vec{P}_{1,z}\rangle \\ .. & .. & .. \\ |\vec{P}_{n-1,x}\rangle & |\vec{P}_{n-1,y}\rangle & |\vec{P}_{n-1,z}\rangle \end{pmatrix} \begin{bmatrix} |\vec{S}_0\rangle \\ |\vec{S}_1\rangle \\ .. \\ |\vec{S}_{n-1}\rangle \end{bmatrix} \quad (2.0)$$

Equation 2.0 says that any object in remote sensing data with time fluctuations can be represented in hyperpatches,[15] which are illustrations of surface and transferred curve frames over a fluctuation period.[16] Let's assume that the blend control point matrix is $|\vec{N}_{n\times 3}\rangle$ and the formation fluctuation periodic knots planes are $|O_i\,(u)\rangle,|O_j\,(v)\rangle,|O_k\,(w)\rangle,$and$|\,O_l\,(t)\rangle$ and lastly $|I\rangle,|J\rangle,|K\rangle,$ and $|l\rangle$ are the total number of knot reference frames of the curve space and periodical fluctuations from the original frame to the transferred reference frames. Therefore, the Marghany-4D ( $|\vec{M}_{4D}\rangle$ ) object reconstruction is then formulated as:

$$|\vec{M}_{4D}\rangle = \sum_{i=1}^{I}\sum_{j=1}^{J}\sum_{k=1}^{K}\sum_{l=1}^{L}|\vec{C}(t)_{ijkl}\rangle|\vec{O}_i(\vec{S}_u)\rangle|\vec{O}_j(\vec{S}_v)\rangle|\vec{O}_k(\vec{S}_w)\rangle|\vec{O}_l(t)\rangle \quad (3.0)$$

Following the procedures of Amini et al.[17] the $|\vec{M}_{4D}\rangle$ order summation can be changed as obtained more efficient approaches to simulate multi-dimensional $|\vec{M}_{4D}\rangle$ consequences. To this end, HRSC frames data are accounted into 300 frames with 30 iterations to obtain a fitting algorithm, which took 588 seconds for every 6 frames of HRSC data.

The general algorithm to transfer from three to four dimensions using $|\vec{M}_{4D}\rangle$ is straightforward, the quantity of factors for these circumstances is 60, 140, 280, and 504, respectively. In other words, quantity of factors for order *O* is $(O + 1)(O + 2)(O + 3)(O + 4) / 6$. In these regards, the considered number of four-dimensional is the fifth-order codes of $25^{504}$, where a number is also huge to judge to whatever consequential; it perhaps also be infinite.

## Results and discussions

Figure 3 shows the Mars craters within the Hellas Basin that were acquired on 17 December 2013 by HRSC camera on the location of Meridiani Planum. Therefore, 3.8 to 4.1 billion years ago, these series of Hellas basins are created post an inordinate asteroid stroke the red planet surface. These series of Hellas basins are then revised by the influences of the activities of wind, ice, water, and volcanic meanwhile they were shaped out. Farther than that, HRSC was proficient to visualize the craters in the ground- resolution is approximately 15 m per pixel with 25 Km across the image coverage. In this regard, 25 km across is the size of two imagined largest craters using HRSC. Consequently, the morphology of numerous topographies in the Hellas Basin and its backgrounds intensely recommends the existence of ice and glaciers; respectively. In this scene, the HRSC sensor delivers a clear 3-D geological features map of Mars owing to the high-resolution stereo head operating on push-broom mode. In this understanding, sensors imagine a line on the Mars surface upright to the milled track of the spacecraft and count on the orbital motion of the spacecraft to shift them as they imagined image sequences recognized as an image swath data.[5,6]

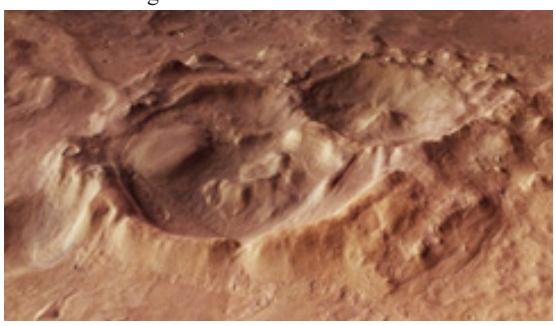

**Figure 3** 3-D crater image acquired by HRSC camera.

Figure 4 confirms liquid flow features in multidimensional space, which can be perceived exterior the huge crater, which is mainly presented as a four-dimensional geometrical pattern. The 4-D flow was constructed by the M-4D algorithm that designates that the evidence of such substances flowed out from the major crater's circumference into the next a smaller one. Additionally, the M-4D algorithm involves countless polygon patterns, which are allowed to revise into 4-D geometrical form as compared to the ones illustrated in Figure 3. It perhaps indicates the continuation of the water basin. Indeed, in the gravest portions of the basin, the atmospheric pressure is approximately 89% greater than at the carter surface, which may even recommend suitable circumstances for existing of an abundant amount of water. Consequently, Marghany's four-dimensional algorithm (M-4D) proposes that approximately craters in Hellas possibly will comprise water-ice glaciers numerous hundred meters thick, buried beneath several deposit dust layers which agrees with the report delivered by ESA.[18]

Figure 5 shows the Marghany four-dimensional algorithm (M-4D) of carter on Mars, which discriminates between the morphology of both larger and small carters. In addition, 4-D suggests a turbulent

**Citation:** Marghany M. Four-dimensional algorithm for studying geological features on mars using high-resolution stereo camera. *Phys Astron Int J.* 2022;6(2):38–42. DOI: 10.15406/paij.2022.06.00248

pattern flow which is pronounced by irregular polygon patterns which are visualized in 4-D (Figure 5b). Therefore, Marghany's four-dimensional algorithm (M-4D) is divided the 3-D objects from HRSC data into hyperpatches. Consequently, the hyperpatches are signified using surfaces and curves. Then, the surface is described by locating one of the 3-D components to a constant integer value which is the defining the surfaces of hyperpatches.

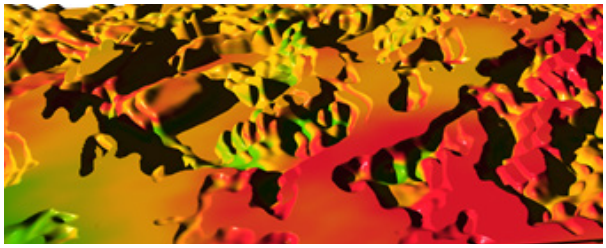

**Figure 4** 4-D flow features using M-4D algorithm.

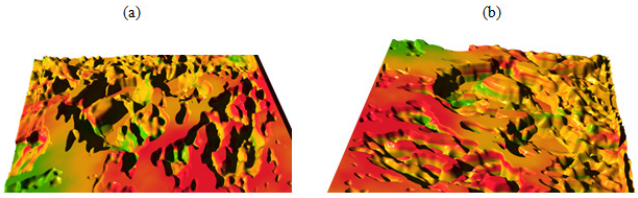


**Figure 5** Marghany's four-dimensional algorithm (M-4D) of Mars carter with different angle views of (a) 180° and (b) 85°.

The energy of the Marghany four-dimensional algorithm (M-4D) is circumscribed as the sum of every knot's weight energy, which is pronounced as the integral of the equivalent potential completed on the knot level surface, which positively approves the study of Waks et al.[19] The Marghany four-dimensional algorithm (M-4D) is constructed on the control knots of a 4-D grid. Consequently, algorithm energy is the function of all control knots which is related to frames of HRSC data. Entirely knot planes are improved despite the potential role of a function being split. The Marghany four-dimensional algorithm (M-4D) process is stopped since the threshold is larger than the length. This study supports the work of Marghany[20] which is based on 4-D reconstruction from hologram interferometry. It can be said Marghany's four-dimensional algorithm (M-4D) holds promises to implement the concept of 4-D in remote sensing applications and space technology too. Such Mars studies are required to be presented in high dimensions to acquire precise information on how the Mars features have deformed over billion of years.

## Conclusion

The core involvement of this investigation is to develop a novel algorithm in 4-D geometrical features reconstruction, which is mainly known as the Marghany four-dimensional algorithm (M-4D). To this end, 3-D data of HRSC was acquired and then Marghany's four-dimensional algorithm (M-4D) was employed sequences of periodical HRSC data in a different frame of time and spaces. The study reveals that the M-4D algorithm can trace the 4-D liquid flow shape which could be proof of water's existence in the red planet. The existence of water, the 4-D visualization of the Marghany four-dimensional algorithm (M-4D) shows a great tectonic associated with a volcanic eruption. In conclusion, integration between the Marghany four-dimensional algorithm (M-4D) and the HRSC can be a promised tool for carter's 4-D reconstruction.

## Acknowledgments

None.

## Conflicts of Interest

None.

## References

1. Martin LJ, PB James, A Dollfus, et al. Telescopic observations: Visual, photographic, polarimetric, in Mars , edited by HH Kieffer, BM Jakosky, MS Matthews, Univ. of Ariz. Press, Tucson 1992;pp. 34–70.
2. de Vaucouleurs G. Physics of the Planet Mars. Faber and Faber, London, 1954.
3. Mutch TA, RE Arvidson, JW Head, et al. The Geology of Mars, Princeton Univ. Press, Princeton NJ.
4. Rencz AN. Remote sensing for the earth sciences: manual of remote sensing 3(No. Ed. 3). John Wiley and sons, 1967.
5. Carr M. The surface of Mars. Cambridge, UK: Cambridge University Press, 2006.
6. Hartmann W. A Traveler's Guide to Mars: The Mysterious Landscapes of the Red Planet. New York: Workman Publishing, 2003.
7. Evans LG, RC Reedy, JI Trombka. Introduction to planetary remote sensing gamma ray spectroscopy, in Remote Geochemical Analysis: Elemental and Mineralogic Composition, C.M. Pieters and P.A.J. Englert, eds., Cambridge Univ. Press, 1993;pp.167–198.
8. Yin LI, JI Trombka I Adler, M Bielefeld. X –ray remote sensing techniques for geochemical analysis of planetary surfaces, in Remote Geochemical Analysis: Elemental and Mineralogic Composition, C.M. Pieters and P.A.J. Englert, eds., Cambridge Univ. Press, 1993;pp., 199–212.
9. Burns RG. Origin of Electronic Spectra of Minerals in the Visible – Near Infrared Region. In Remote Geochemical Analysis: Elemental and Mineralogical Composition, ed. C.M. Pieters and P.A.J. Englert, Cambridge: Cambridge Univ. Press.1993;pp.3 –29.
10. Gaffey SJ, LA McFadden, DB Nash. Ultraviolet, visible, and near –infrared reflectance spectroscopy: Laboratory spectra of geologic materials. InRemote Geochemical Analysis: Elemental and Mineralogical Composition, CM Pieters, PAJ Englert, eds., pp. 43 –71. Cambridge: Cambridge Univ. Press. 1993.
11. Christensen PR. The spatial distribution of rocks on Mars. *Icarus.* 1986;68:217–238.
12. Kahle AB, FD Palluconi, PR Christensen. Thermal emission spectroscopy: Application to the Earth and Mars, in Remote Geochemical Analysis: Elemental and Mineralogical Composition. C.M. Pieters and P.A.J. Englert, eds., Cambridge Univ. Press, 1993;pp.99–120.
13. Shelley C. NASA's Great Observatories. NASA. 2008.
14. Marghany M. Nonlinear Ocean Dynamics: Synthetic Aperture Radar. Elsevier, 2021.
15. Mortenson ME.1985,Geometric Modeling. John Wiely& sons, NewYork, 1985.
16. Amini AA, P Radeva, D Li. Measurement of 3D motion of myocardial material points from explicit B –surface reconstruction of tagged data", Medical Image Computing and Computer –Assisted Intervention, MIT, Cambridge, MA, October 1998b.
17. Amini AA, Y Chen, RW Curwen, et al. Coupled B –Snake Grids and Constrained Thin –Plate Splines for Analysis of 2 –D Tissue Deformations from Tagged MRI". *IEEE Transactions on Medical Imaging.* 1998a:17(3):344 –356.

18. ESA 2015, Craters within the Hellas Basin.

19. Waks E, Prince J, Douglas A. Cardiac Motion Simulator for Tagged MRI. *Mathematical Methods in Biomedical Image Analysis.* 1996;182–191.

20. Marghany M. Hologram interferometric SAR and optical data for fourth –dimensional urban slum reconstruction. Proceedings of 35 th Asian conference on remote sensing. Nay Pyi Taw, Myanmar 1994;27–31.

21. [Access on August 20 2015].

22. Radeva P, Amini A, Huang J. Deformable B –Solids and Implicit Snakes for 3D Localization and Tracking of SPAMM MRI Data. *Computer Vision and Image Understanding.* 1997;66:163–178.

23. Sheehan W. Planets and Perception, Univ. Arizona Press. 1988.

**Citation:** Marghany M. Four-dimensional algorithm for studying geological features on mars using high-resolution stereo camera. *Phys Astron Int J.* 2022;6(2):38–42. DOI: 10.15406/paij.2022.06.00248